Crystal growth / Croissance cristalline

Growth and characterizations of lead-free ferroelectric KNN-based crystals

Cristallogenèse et caractérisations de monocristaux ferroélectriques sans plomb à base de KNN

Mythili Prakasam [a], Philippe Veber [a,*], Oudomsack Viraphong [a], Laetitia Etienne [a], Michel Lahaye [a], Stanislav Pechev [a], Eric Lebraud [a], Kiyoshi Shimamura [b], Mario Maglione [a]

[a] *ICMCB Université de Bordeaux, CNRS, 87, avenue du Docteur-Albert-Schweitzer, 33608 Pessac cedex, France*
[b] *National Institute for Materials Science (NIMS), 1-1 Namiki, Tsukuba, Ibaraki, 305-0044, Japan*

A B S T R A C T

We have grown by flux method centimeter-sized single crystals from pseudo-hexanary Li_2O–Na_2O–K_2O–Nb_2O_5–Ta_2O_5–Sb_2O_3 system. Based on chemical analysis, crystals of compositions $(Li_{0.023}Na_{0.583}K_{0.394})(Nb_{0.925}Ta_{0.037}Sb_{0.038})O_3$ and $(Li_{0.034}Na_{0.609}K_{0.357})(Nb_{0.896}Ta_{0.047}Sb_{0.057})O_3$ were characterized by X-rays diffraction which revealed a tetragonal structure. The dielectric analysis confirmed that the ferroelectric behavior of these crystals is very sensitive to little changes in composition as previously observed on ceramics. Such high flexibility of the ferroelectric properties in crystals opens the way towards improved understanding of the relations between structure and polarization in solid solutions which may be an alternative to the lead-based materials.

© 2012 Académie des sciences. Published by Elsevier Masson SAS. All rights reserved.

R É S U M É

Des monocristaux centimétriques issus du système Li_2O–Na_2O–K_2O–Nb_2O_5–Ta_2O_5–Sb_2O_3 ont été obtenus par la méthode des flux. Les cristaux de composition $(Li_{0.023}Na_{0.583}K_{0.394})(Nb_{0.925}Ta_{0.037}Sb_{0.038})O_3$ et $(Li_{0.034}Na_{0.609}K_{0.357})(Nb_{0.896}Ta_{0.047}Sb_{0.057})O_3$ ont été caractérisés par diffraction des rayons X et se sont avérés appartenir au système quadratique. Leur comportement ferroélectrique spécifique a été confirmé par des mesures diélectriques. Une telle flexibilité des propriétés ferroélectriques de ces cristaux pour de faibles variations de composition ouvre la voie vers une meilleure compréhension des relations entre la structure et la polarisation dans ces solutions solides, qui sont potentiellement une alternative aux matériaux contenant du plomb.

© 2012 Académie des sciences. Published by Elsevier Masson SAS. All rights reserved.

1. Introduction

Ferroelectric perovskite are of great importance among all the currently probed piezoelectric materials. The structure has a general formula ABO_3 and is described as a cubic unit cell with the corners occupied by a large cation ("A", such as Pb,

---

Ba, Ca, K, Na, etc.), the center by a smaller cation ("B", such as Ti, Nb, Mg, Zr, etc.) and oxygen in the faces center. Owing to the increased focus on the research of environment friendly ferroelectric materials, there is an urge to replace lead-based ferroelectric and piezoelectric materials. $(K_{0.5}Na_{0.5})NbO_3$(KNN) is one of the promising materials with the possibility to replace $Pb(Zr,Ti)O_3$(PZT) because of its good piezoelectric properties and high Curie temperature [1–4]. Various synthesis methods are focused in order to process the pure KNN materials in the form of ceramics. However, difficulties, such as their densification through the conventional solid state reaction method and poling process, were observed [5–7].

Solid solutions of KNN doped with various ABO_3 type materials, such as $BaTiO_3$ [8], $SrTiO_3$ [9], $LiSbO_3$ [10] and $LiTaO_3$ [11–13] have been investigated in order to improve piezoelectric properties of KNN-based material as well as its Curie temperature. In the KNN-$LiNbO_3$ system [14–20], the piezoelectric property enhancement is induced by $LiNbO_3$ [14,16] or by changing the sintering temperature [18]. Recently, the effects of alkali metals content were reported underlining the change of the structure from tetragonal to orthorhombic phase [21,22]. In order to enhance the piezoelectric properties of this material, one possible way could be to grow by a solid state growth method KNN-based ceramics with oriented grains along certain crystallographic directions, as has been demonstrated for the case of $KNbO_3$ by Wada et al. [23] and for relaxor-based ferroelectric single crystals by Park et al. [8] and Shrout et al. [12]. So far, researchers [24–26] have used solid state single crystal growth methods for growing alkali niobate-based single crystals. Still poor reproducibility related to compositional inhomogeneities is experienced [27,28]. Controlling a constant amount of the alkali elements in the compound imposed severe difficulty in handling KNN-based materials.

Based on previous investigations on ceramics, we chose KNN solid solutions doped with $LiNbO_3$ where niobium was substituted by antimony and tantalum as referenced by Saito et al. [1] in order to reach the Morphotropic Phase Boundary (MPB) composition where high and stable piezoelectric characteristics are expected. Hence, as referenced by Fu et al. [29] $(Li_xNa_{0.52}K_{0.48-x})(Nb_{1-x-y}Ta_xSb_y)O_3$ composition with $x = 0.04$ and $y = 0.06$ is considered for its large piezoelectric coefficients ($d_{33} = 335$ pC N^{-1}) and high Curie temperature ($T_c = 291\,^\circ$C).

Compared to these previous investigations on ceramics, single crystals can lead to better chemical homogeneities control and improved understanding of the crystalline structure. As evidenced in the case of lead-containing piezoelectrics, this is a key step towards the improvement of the piezoelectric performances. In the present work, we thus have grown and characterized $Li_2O-Na_2O-K_2O-Nb_2O_5-Ta_2O_5-Sb_2O_3$ solid solutions (KNLSTN) in the vicinity of MPB in order to clear the way for understanding their ferroelectric/piezoelectric properties. Single crystals of various compositions have been grown from high temperature solutions. We focused our attention on finding the crystalline symmetry for various Li/Na/K ratio correlated with the dielectric properties of single crystals. As-grown crystals were chemically analyzed and our dielectric investigations on single crystals with compositions $(Li_{0.023}Na_{0.583}K_{0.394})(Nb_{0.925}Ta_{0.037}Sb_{0.038})O_3$ and $(Li_{0.034}Na_{0.609}K_{0.357})(Nb_{0.896}Ta_{0.047}Sb_{0.057})O_3$ show a good indication of ferroelectricity. The correlation of the crystalline symmetry, chemical content and ferroelectricity is undertaken and the results are discussed in detail.

2. Experimental procedure

2.1. Crystal growth

Five growth attempts, numbered from $i = 1$ to 5, are presented. To our knowledge, there are no data in literature dealing with phase relations and single crystal growth in the pseudo-hexanary $Li_2O-Na_2O-K_2O-Nb_2O_5-Ta_2O_5-Sb_2O_3$ system and no crystal growth with Sb_2O_3 have been studied so far. Nevertheless, we noted that numerous crystal growths of $Li_2K_3(Nb/Ta)_5O_{15}$ (KLN/KLT) defined compound or solid solutions from various alkali–niobium–tantalum oxides-based pseudo-ternary and pseudo-quaternary systems have been undertaken [30–52]. Crystal growth experiments were carried out mainly with a self-flux method using alkali oxides rich-solutions such as K_2O-Li_2O. Lithium–sodium-based flux such as NaF, mixture of LiF–NaF or with $NaBO_2$ with various amounts of alkali, niobium and tantalum oxides are also reported. Previous experiments on the $A_2O-Nb_2O_5$ (with A = Na or K) pseudo-binary systems have revealed a number of phases with different A_2O/Nb_2O_5 ratios in addition to the perovskite phase. Hence additional phases other than perovskite solid solutions would form in the reaction between K_2O, Na_2O and Nb_2O_5. Furthermore, maintaining the stoichiometry is extremely difficult due to the alkali-based compounds volatilization at the processing temperature required for crystal growth. Moreover, different diffusion rates of the sodium and potassium species could lead to local inhomogeneities in the solid solution. It has to be noted that Li, Ta and Sb increase the melting or the saturation temperature enhancing thus the volatilization of the alkali-based liquid solution. Thermal fluctuations at solid–liquid interface may lead to incorporation of defects and flux inclusions within the crystal during the growth. Hence a tricky temperature control for crystal growth is required for this type of compounds. The crystal growth from high temperature solution is considered for KNLSTN system. K_2O and Li_2O mixture which act usually as main components for self-flux for the growth as previously described is then chosen.

In present work, the total amount of oxides present in the bath which includes the solute and its solvent was considered and $(Li_{0.040}Na_{0.520}K_{0.440})(Nb_{0.900}Ta_{0.040}Sb_{0.060})O_3$ [30] represents the solute to be grown. As a first assumption for attempt $i = 1$, we considered that segregation coefficients depend on molar fraction of each element with respect to A or B sites as deduced from previous works [30–48]. Indeed, effective segregation coefficients of elements with respect to their molar fractions were either given or calculated and have shown a good reliability between them. Thus the average segregation coefficients for the considered KNLSTN composition were chosen following: $k_{Li} = 0.2$ [33]; $k_{Na} = 1.8$ [32,41]; $k_K = 0.25$ [32]; $k_{Nb} = 0.75$ [38,43,45,46] and $k_{Ta} = 3.5$ [43,45,46] in order to reach the MPB. Antimony segregation coefficient was

Table 1
Normalized liquid compositions of the crystal growth attempts.

Liquid *i* composition (normalized)	%mol. Li	%mol. Na	%mol. K	%mol. Nb	%mol. Ta	%mol. Sb
1	8.9%	12.8%	78.3%	96.7%	0.9%	2.4%
2	10.3%	40.8%	48.9%	78.6%	1.5%	19.9%
3	11.4%	27.1%	61.5%	89.8%	1.3%	8.9%
4	11.4%	22.8%	65.8%	91.9%	1.5%	6.6%
5	11.4%	21.3%	67.3%	91.9%	1.5%	6.6%

assumed to be equal to 2. The molar composition of the load for the first attempt was thus calculated in order to reach single crystals with the expected MPB composition and was normalized in accordance with the stoichiometric KNLSTN formula. Molar composition of the liquid bath for attempts $i = 2$ to 5 were deduced in a similar way from the polynomial regression fitted curve deduced from the chemical analysis performed on crystals grown from the previous attempts as a function of the liquid composition. Liquid compositions of the five growth attempts are given in Table 1. Alkali content was steadily varied and kept nearly constant for attempt $i = 3$ to 5 in order to characterize the influence of volatilization with respect to its incorporation in the crystals.

Synthesis of KNLSTN was performed by high temperature solid-state reaction using oxide powders of Na_2CO_3 (99.99%), Li_2CO_3 (99.99%), K_2CO_3 (99.99%), Nb_2O_5 (99.99%), Ta_2O_5 (99.99 %), and Sb_2O_3 (99.99%). The raw materials were mixed together by ball milling with ethanol as the binder. The mixture was then heated in a platinum crucible up to 450 °C for 12 h under air atmosphere and then raised up to 800 °C for 12 h with a rate of 120 °C h^{-1} and finally molten at a temperature above 1200 °C. The charge was held at a soaking temperature which is about 20 °C above the saturation temperature and stirred continuously with a platinum spatula at a rate of 40 rpm for 24 h under air atmosphere. Crystal growth was carried out in a two-zone resistive heating furnace with a longitudinal thermal gradient less than 1 °C cm^{-1}. A platinum wire was used as the nucleation site for the crystal growth and a weighing device was used in order to measure the weigh loss of the load in the crucible as well as the mass of growing crystals. The rotation speed was set between 8 rpm and 20 rpm and decreasing thermal ramps ranging between 0.1 °C h^{-1} and 1 °C h^{-1} were programmed.

2.2. Characterization

Powder XRD were performed using a PANalytical X'Pert Pro MPD diffractometer in $\theta - 2\theta$ Bragg–Brentano geometry with a primary germanium (111) monochromator for pure Cu–K$_{\alpha 1}$ radiation working at 45 kV and 40 mA and equipped with a spinner.

Electron Probe Micro Analysis (EPMA) was achieved on as-grown crystals with a CAMECA SX-100 apparatus with a wavelength dispersive spectrometer working at 15 kV and 10 nA. In addition, chemical analysis were done with a VARIAN 720-ES Inductively Coupled Plasma Optical Emission Spectroscopy (ICP-OES) set up. Samples weighing $\sim$ 20 mg were dissolved in 10 ml mixture of HF(48%)–HNO$_3$(68%)–HCl(38%) with volume ratio 1:3:3 respectively and 90 ml of distilled water. ICP-OES and EPMA analysis were performed in different regions of several samples from the same attempt and given element concentration were averaged. Absolute accuracy for Li content measured by ICP-OES was calculated around 0.24 mol.%. The whole measurements performed on other elements led to an absolute concentration accuracy of about 0.5 mol.% for alkali elements (Na and K), less than 0.4 mol.% for Nb and Sb, and less than 0.1 mol.% for Ta. Cut and polished parallel plate crystals of (001)-oriented KNLSTN crystals with average dimensions 1×5 mm^2-wide and 1 mm-thick were used for dielectric experiments. The major faces were electroded using gold sputtering and silver wires were attached to these electrodes using silver paste. The sample was set in a homemade cell enabling the temperature to be scanned from 80 K up to 500 K. Prior to such low temperature run, the cell was pumped down and a slight overpressure of dry Helium was introduced so as to avoid moisture adsorption. The sample was electrically connected to the output port of a HP4194 impedance analyzer with an operating frequency range of 100 Hz–10 MHz.

3. Results and discussion

Millimeter to centimeter-sized crystals, agglomerated to the platinum wire with large regions devoid of flux, were obtained (Fig. 1). The crystals exhibit clear region with a progressive brownish–orange color deepening with increasing distance from the platinum rod for attempts 1 and 2. Crystals obtained from attempts 3 to 5 show clear region and white cloudy regions randomly distributed. Saturation temperature, duration of growth and weight percentage of volatilization with respect to the initial load are given in Table 2.

3.1. Chemical analysis of KNLSTN crystals

Chemical analyses of as-grown crystal are given in Table 3 and it can be inferred that the crystal growth $i = 1$ has shown a composition diverging significantly from expected MPB composition. Volatilization rate (see Table 2) was quite low

Fig. 1. Examples of centimeter-sized as-grown crystals obtained from attempts $i = 1$ (a), $i = 3$ (b) and $i = 5$ (c).

Table 2
Saturation temperatures, crystal growth durations and weight losses percentage of volatilization with respect to the attempts.

Attempt i	$T_{saturation}$ (°C)	% weight loss	Duration of growth (h)
1	885	3%	200
2	1195	5%	250
3	1190	< 2%	100
4	1200	7%	250
5	1200	< 1%	50

Table 3
Chemical analysis of the as-grown crystals.

Crystal composition i	%mol. Li	%mol. Na	%mol. K	%mol. Nb	%mol. Ta	%mol. Sb
1	2.0%	15.5%	82.5%	97.9%	0.7%	1.4%
2	3.4%	84.7%	11.9%	86.8%	4.0%	9.1%
3	2.5%	55.8%	41.7%	92.6%	2.4%	5.0%
4	2.3%	58.3%	39.4%	92.5%	3.7%	3.8%
5	3.4%	60.9%	35.7%	89.6%	4.7%	5.7%

due to low saturation temperature, even if the growth duration was long, implying that segregation is governed mainly by the nature of the solid solution in the phase diagram. Segregation of each element with respect to the others in their respective site in the crystals has to be taken into account. Actually, in the case of KNLSTN, three elements are present per site involving a competition between ions as for their incorporation in the crystal lattice contrary to the assumption done in Section 2.1 which took into account only two ions per site. Segregation of elements in KNLSTN system for the five attempts of growth are shown in Fig. 2 where molar fraction of elements in as-grown crystal is plotted as a function of their initial compositions in the load.

Volatilization rates showed that the durations of growth with respect to the saturation temperature have an important role in the incorporation of alkali elements in A site and of antimony in B site. Volatilization rate is related to the weight percentage losses of the liquid bath as given in Table 2. It depends both on growth duration as shown by attempt 2 and 3 for which saturation temperatures are very close and on the saturation temperature as shown for attempt 1 and 2 for which the durations of growth are close. Comparison between attempts 4 and 5 for which the growth times was decreased by a factor five, reveals that the molar relative variations of Li, K, Ta and Sb contents are respectively 32%, 10%, 22% and 32% whereas other ions (Na and Nb) contents remain steady. It is obvious that the volatilization depends both on the saturation temperature and growth duration. While a smaller deviation in the compatibility between the ICP-OES and EPMA could be due to probable flux inclusions in the crystal and also to the variations of compositions of solid solutions observed overall in the single crystal, we noticed a rather good matching between values obtained between both chemical analysis techniques for alkali metal (Na and K) concentrations. We conclude that effective segregation of alkali element is strongly dependent on the rate of volatilization of the bath. The control of stoichiometry of alkali elements, especially lithium, as well as antimony, is tricky to set due to the high saturation temperature (around 1200 °C) by comparison with the low melting point of K_2O ($T_m = 763$ °C) which is the main component of the solvent (> 75 mol.%).

3.2. Dielectric and XRD analysis of KNLSTN

The dielectric measurements were carried out on all the samples from 1–5. Since no dielectric anomaly was found on samples 1 to 3, the results of samples 4 and 5 showing their ferroelectric properties are discussed in this section with respect to XRD measurements.
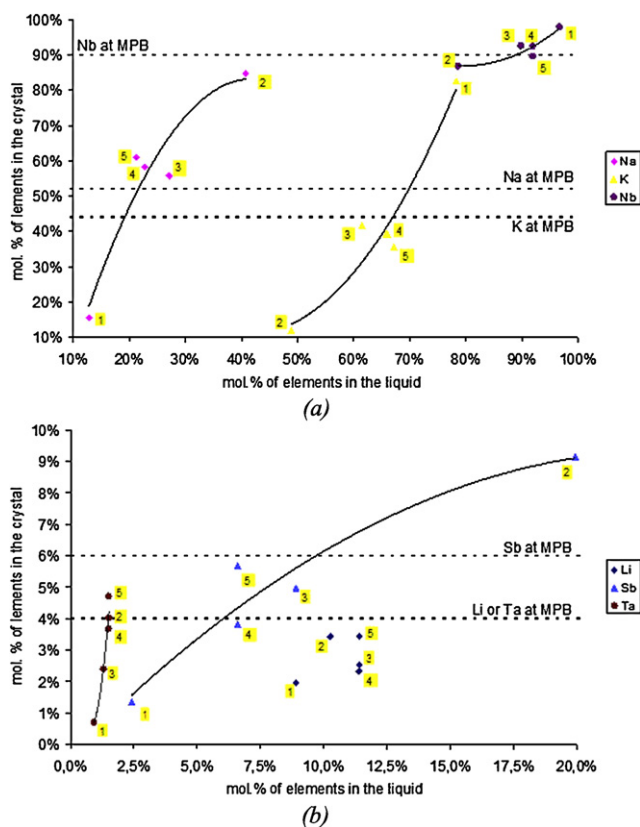
Fig. 2. Segregation of elements in KNLSTN system where the number of considered attempt i ($i = 1$ to 5) is written with yellow background. (a) mol.% concentration of Na, K and Nb elements in crystal as a function of their initial one in liquid bath. (b) mol.% concentration of Li, Sb and Ta elements in crystal as a function of their initial one in liquid bath. The dashed lines show the targeted compositions for which optimal piezoelectric coefficients are expected [29]. (For interpretation of the references to color in this figure, the reader is referred to the web version of this article.)

The temperature dependence of the dielectric constant is shown in Fig. 3. While two peaks are observed at 370 °C and 160 °C for sample 4, only one single ferroelectric transition was recorded on sample 5 at 250 °C. All these anomalies can be ascribed to ferroelectric transitions because they are frequency independent and the divergence of the dielectric permittivity could be fitted to a Curie–Weiss law $\varepsilon(T) = C/(T - T_c)$. In sample 5 the extrapolated Curie temperature was found to be 248 °C, close to the temperature of the dielectric maximum of 250 °C. This confirms that the ferroelectric transition is of a second order type.

KNLSTN ceramics of composition close to our single crystals exhibit two phase transition temperatures, an orthorhombic (O) to tetragonal (T) transition temperature $T_{(O\text{-}T)}$ at around 200 °C and tetragonal to cubic (C) transition temperature $T_{(T\text{-}C)}$ at 400 °C [53]. These are close to our reported transition temperatures in sample 4 where $T_{(O\text{-}T)} = 160$ °C and $T_{(T\text{-}C)} = 370$ °C and for which a deficit of lithium has been observed. We thus confirm that KNLSTN single crystals have the same succession of phase transition than ceramics of the same composition. We next compare the ferroelectric transition temperature of samples 4 and 5. We see a down-shift of the first transition temperature $T_{(T\text{-}C)}$ of more than 100 °C in sample 5. From the chemical analysis reported above, the main trend is that sample 5 includes more Li than sample 4 (3.4 mol.% instead of 2.2 mol.%). Such strong depression of ferroelectric transition temperature upon increasing Li substitution was also reported by Jimenez et al. [54] in ceramics where larger amount of Li in the starting reagents was needed in order to get such a large transition temperature shift. In addition, Hollenstein et al. [15] and Ochoa et al. [55] found that the addition of Li in the A site and Ta, Sb in the B site in ceramics decrease this temperature.

The powder XRD patterns of crushed KNLSTN single crystals corresponding to attempts 4 and 5 depicted in Figs. 4(a) and 4(b) exhibit diffraction peaks corresponding to perovskite phase [56,57]. Both patterns of Fig. 4(c) are consistent with tetragonal state but the shifting of the (002) line towards low angles is highly sensitive to little change of compositions. Following Fu et al. [29], we note that samples 4 and 5 are close to the switching between orthorhombic and tetragonal symmetry at room temperature. As a consequence, the ferroelectric behaviors of samples 4 and 5 are drastically different as can be seen from the sizable differences in transitions temperatures (Fig. 3). No parasitic phases such as KLN or KLT defined compounds were found as previously shown by Rubio et al. in sintered ceramics [56,57]. The single crystals 4 and 5 in the present work have thus similar behavior compared to ceramics of the same composition. The large change of ferroelectric transition temperature with minute change of composition is similar to what is observed in the morphotropic region of lead
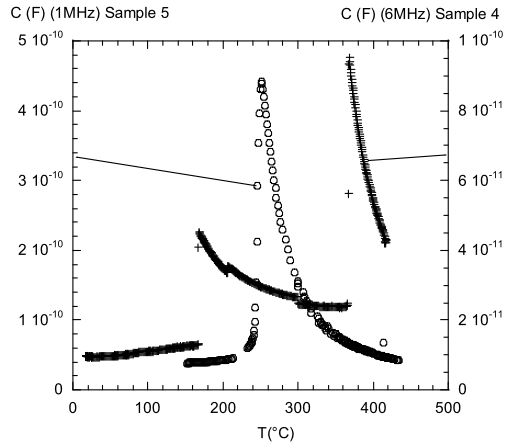
Fig. 3. Variation of dielectric properties with temperature for sample 4 and 5.
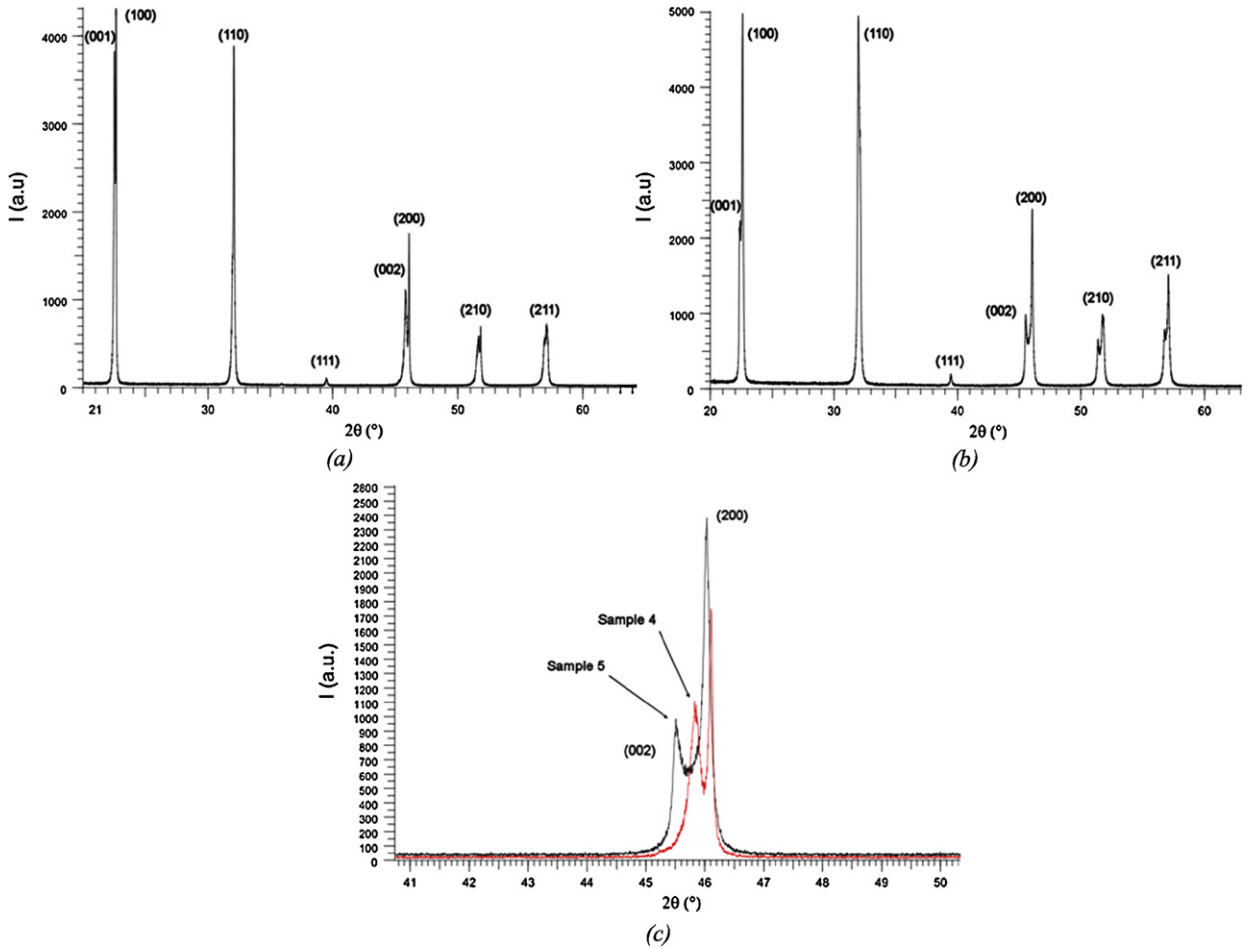
Fig. 4. XRD patterns on crushed crystals for sample 4 (a) and sample 5 (b) exhibiting tetragonal structure. (c) Zoom on (200) and (002) lines.

containing materials like PZT [58] or lead-free BCTZ [59] solid solutions where a triple point is expected. This similarity is an indication for possible large piezoelectric coefficients of KNLSTN single crystals, but this is still remaining an open question.

4. Conclusion

Centimeter-sized KNLSTN single crystals have been successfully grown by flux method. EPMA and ICP-OES analysis were performed on as-grown crystals confirming the huge loss of the alkali compounds, particularly lithium with respect to the duration of growth. In addition, the loss of antimony has been evidenced as observed in other KNN-LiSbO$_3$ based systems. Two single crystals (Li$_{0.023}$Na$_{0.583}$K$_{0.394}$)(Nb$_{0.925}$Ta$_{0.037}$Sb$_{0.038}$)O$_3$ and (Li$_{0.034}$Na$_{0.609}$K$_{0.357}$)(Nb$_{0.896}$Ta$_{0.047}$Sb$_{0.057}$)O$_3$ with close compositions have shown two types of sharp different dielectric features which have been correlated to the change of structure. While XRD analysis identified the presence of pure perovskite phase with tetragonal symmetry in both samples, first sample exhibited ferroelectric responses like orthorhombic structure and characterized by a dielectric transitions at around $T_{(O-T)} = 160\,^\circ$C and then a ferroelectric to paraelectric one measured at $T_{(T-C)} = 370\,^\circ$C. Second sample displayed one ferroelectric to paraelectric transition at $T_{(T-C)} = 248\,^\circ$C. Our research team will present the further piezoelectric results on KNLSTN single crystals in near future.

Acknowledgement

References

[1] Y. Saito, H. Takao, T. Tani, T. Nonoyama, K. Takatori, T. Homma, T. Nagaya, M. Nakamura, Nature 84 (2004) 432.
[2] H.-G. Yeo, Y.-S. Sung, T.K. Song, J.-H. Cho, M.-H. Kim, T.-G. Park, J. Korean Phys. Soc. 54 (2009) 896.
[3] J. Abe, M. Kobune, K. Kitada, T. Yazawa, H. Masumoto, T. Goto, J. Korean Phys. Soc. 51 (2007) 810.
[4] T.K. Song, M.-H. Kim, Y.-S. Sung, H.G. Yeo, S.H. Lee, S.-J. Jeong, J.-S. Song, J. Korean Phys. Soc. 51 (2007) 697.
[5] V.J. Tennery, K.W. Hang, J. Appl. Phys. 39 (1968) 4749.
[6] D.H. Cho, M.K. Ryu, S.S. Park, S.Y. Cho, J.G. Choi, M.S. Jang, J.P. Kim, C.R. Cho, J. Korean Phys. Soc. 46 (2005) 151.
[7] L. Egerton, D.M. Dillon, J. Am. Ceram. Soc. 45 (1959) 438.
[8] H.Y. Park, C.W. Ahn, H.C. Song, J.H. Lee, S. Nahm, K. Uchino, H.J. Lee, Appl. Phys. Lett. 89 (2006) 062906.
[9] V. Bobnar, J. Bernard, M. Kosec, Appl. Phys. Lett. 85 (2004) 994.
[10] S. Zhang, R. Xia, T.R. Shout, G. Zang, J. Wang, J. Appl. Phys. 100 (2006) 104108.
[11] Y. Dai, X. Zhang, G. Zhou, Appl. Phys. Lett. 90 (2007) 262903.
[12] T.R. Shrout, S.J. Zhang, J. Electroceram. 19 (2007) 113.
[13] B. Jaffe, W. Cook, H. Jaffe, Piezoelectric Ceramics, Academic, New York, 1971, p. 136.
[14] Y. Guo, K. Kakimoto, H. Ohsato, Appl. Phys. Lett. 85 (2004) 4121.
[15] E. Hollenstein, M. Davis, D. Damjanovic, N. Setter, Appl. Phys. Lett. 87 (2005) 182905.
[16] H.L. Du, W.C. Zhou, F. Luo, D.M. Zhu, S.B. Qu, Z.B. Pei, Appl. Phys. Lett. 91 (2007) 202907.
[17] H.C. Song, K.H. Cho, H.Y. Park, C.W. Ahn, S. Nahm, K. Uchino, S.H. Park, H.G. Lee, J. Am. Ceram. Soc. 90 (2007) 1812.
[18] P. Zhao, B.-P. Zhang, J.-F. Li, Appl. Phys. Lett. 90 (2007) 242909.
[19] P. Zhao, B.-P. Zhang, J.-F. Li, Appl. Phys. Lett. 91 (2007) 172901.
[20] K. Wang, J.-F. Li, Appl. Phys. Lett. 91 (2007) 262903.
[21] S.C. Lee, H.-G. Yeo, J.H. Cho, Y.S. Sung, M.-H. Kim, T.K. Song, S.S. Kim, B.C. Choi, K.-S. Choi, J. Korean Phys. Soc. 56 (2010) 453.
[22] S.C. Lee, L. Wang, H.-G. Yeo, J.H. Cho, Y.S. Sung, M.-H. Kim, T.K. Song, S.S. Kim, B.C. Choi, Ferroelectrics 176 (2009) 381.
[23] T. Wada, K. Tsuji, T. Saito, Y. Matsuo, H. Adachi, Jpn. J. Appl. Phys. 42 (2003) 6110.
[24] M. Davis, N. Klein, D. Damjanovič, N. Setter, Appl. Phys. Lett. 90 (2007) 0629041.
[25] A. Bencan, E. Tchernychova, H. Ursic, M. Kosec, J. Fisher, Growth and characterization of single crystals of potassium sodium niobate by solid state crystal growth, in: Ferroelectrics – Material Aspects, Mickael Lallart Edition, ISBN 978-953-307-332-3, 2011, Chapter 5.
[26] J.G. Fisher, A. Benčan, J. Bernard, J. Holc, M. Kosec, S. Vernay, D. Rytz, J. Eur. Ceram. Soc. 27 (2007) 4103–4106.
[27] P. Bomlai, P. Wichianrat, S. Muensit, S.J. Milne, J. Am. Ceram. Soc. 90 (2007) 1650.
[28] D. Jenko, A. Benčan, B. Malič, J. Holc, M. Kosec, Microsc. Microanal. 11 (2005) 572.
[29] J. Fu, R. Zuo, X. Fang, K. Liu, Mat. Res. Bul. 44 (2009) 1188–1190.
[30] E. Irle, R. Blachnik, B. Gather, Thermochim. Acta 179 (1991) 157.
[31] K. Polgar, A. Peter, L. Kovacs, G. Corradi, Zs. Szaller, J. Cryst. Growth 177 (1997) 211.
[32] A. Reisman, E. Banks, J. Am. Chem. Soc. 80 (1958) 1877.
[33] R. Hofmeister, A. Yariv, A. Agranat, J. Cryst. Growth 131 (1993) 486.
[34] Q. Guan, X. Hu, J. Wei, J. Wang, L. Tian, W. Cui, Y. Liu, J. Cryst. Growth 197 (1999) 1012.
[35] J.J. Van Der Klink, D. Rytz, J. Cryst. Growth 56 (1985) 673.
[36] S. Podlojenov, M. Burianek, M. Mühlberg, Cryst. Res. Technol. 38 (2003) 1015.
[37] J.Y. Wang, Q.C. Guan, J.Q. Wei, M. Wang, Y.G. Liu, J. Cryst. Growth 116 (1992) 27.
[38] A. Reisman, S. Triebwasser, F. Holtzberg, J. Am. Chem. Soc. 77 (1955) 4228.
[39] D. Rytz, PhD thesis n° 475, Ferroélectricité quantique dans KTa$_{1-x}$Nb$_x$O$_3$, Ecole polytechnique federale de Lausanne, 1983.
[40] D. Rytz, H.J. Scheel, J. Cryst. Growth 59 (1982) 468.
[41] M. Badurski, J. Cryst. Growth 46 (1979) 274.
[42] A. Sadel, R. Von der Muhll, J. Ravez, J.P. Chaminade, P. Hagenmuller, Solid State Commun. 44 (1982) 345.
[43] V.I. Chani, K. Nagata, T. Kawaguchi, M. Imaeda, T. Fukuda, J. Cryst. Growth 194 (1998) 374.
[44] T. Fukuda, H. Hirano, J. Cryst. Growth 35 (1976) 127.
[45] T. Fukuda, Jpn. J. Appl. Phys. 9 (1970) 599.
[46] T. Fukuda, H. Hirano, S. Koide, J. Cryst. Growth 6 (1970) 293.
[47] G. Shirane, R. Newnham, P. Pepinsky, Phys. Rev. 96 (1954) 581.
[48] M. Ferriol, M. Cochez, M. Aillerie, J. Cryst. Growth 311 (2009) 4343.
[49] I.P. Raevskii, L.A. Reznichenko, M.P. Ivliev, V.G. Smotrakov, V.V. Eremkin, M.A. Malitskaya, L.A. Shilkina, S.I. Shevtsova, A.V. Borodin, Crystallogr. Rep. 48 (2003) 486.

[50] Z. Zhou, J. Li, H. Tian, Z. Wang, Y. Li, R. Zhang, J. Phys. D: Appl. Phys. 42 (2009) 125405.
[51] H. Tian, Z. Zhou, D. Gong, H. Wang, D. Liu, C. Hou, J. Phys. D: Appl. Phys. 41 (2008) 095105.
[52] Y. Furukawa, S. Makio, T. Miyai, M. Sato, H. Kitayama, Y. Urata, T. Tamiuchi, T. Fukuda, Appl. Phys. Lett. 68 (1996) 744.
[53] B. Jaffe, W. Cook, H. Jaffe, Piezoelectric Ceramics, Academic, New York, 1971.
[54] B. Jiménez, R. Jiménez, A. Castro, L. Pardo, J. Eur. Ceram. Soc. 24 (2004) 1521.
[55] D.A. Ochoa, J.E. García, R. Pérez, V. Gomis, A. Albareda, F. Rubio-Marcos, J.F. Fernández, J. Phys. D: Appl. Phys. 42 (2009) 025402.
[56] F. Rubio-Marcos, P. Ochoa, J.F. Fernandez, J. Eur. Ceram. Soc. 27 (2007) 4125–4129.
[57] F. Rubio-Marcos, P. Marchet, T. Merle-Méjean, J.F. Fernandez, Mater. Chem. Phys. 123 (2010) 91–97.
[58] R. Waser, U. Böttger, S. Tiedke, Polar Oxides, Properties, Characterization, and Imaging, WILEY-VCH Verlag GmbH & Co. KGaA, 2005, p. 139, Chapter 7.
[59] W. Liu, X. Ren, Phys. Rev. Lett. 103 (2009) 257602.